

A Density Functional Study of the Addition of Water to SO₃ in the Gas Phase and in Aqueous Solution

Evert Jan Meijer[†] and Michiel Sprik*

IBM Research Division, Zurich Research Laboratory, CH-8803 Rüschlikon, Switzerland

Received: July 2, 1997; In Final Form: January 5, 1998

The addition of water to sulfur trioxide in liquid water has been studied using the ab initio molecular dynamics (MD) method. The hydration reaction observed in the MD simulation is spontaneous and, within a few hundred femtoseconds, yields a contact ion pair consisting of a hydrogen sulfate anion and a hydronium cation. The reaction mechanism is concerted: sulfur–oxygen bond formation and deprotonation of the hydrating water occur simultaneously. The reaction in solution is compared to two gas-phase additions, namely, the bare reaction with only the two reactants present and the reaction catalyzed by an additional water molecule. Both of these reactions lead to neutral products and require substantial amounts of activation energy. The gas-phase results have also been used to evaluate the accuracy of the BLYP (Becke–Lee–Yang–Parr) functional, which has been used in the ab initio MD to determine the density functional electronic structure. Whereas the calculated geometries of the sulfur trioxide–water complexes SO₃·H₂O and of the reaction product H₂SO₄ are in good agreement with experiment, the formation energies are significantly underestimated, in particular for H₂SO₄.

Introduction

Sulfur trioxide (SO₃) is one of the most reactive species in aqueous solution. Its conversion to sulfuric acid (H₂SO₄) is highly exothermic and occurs almost instantly. In contrast, the addition of water to SO₃ in the gas phase is an activated reaction that proceeds at a much slower rate. The gas-phase reaction is important in the context of atmospheric processes. It is the final stage of the oxidation reaction of sulfur dioxide, which enters the atmosphere mainly through the burning of coal and volcanic activity. Sulfuric acid is the main acid component of acid rain,¹ and it is an important precursor for the formation of atmospheric aerosols. These aerosols play a key role in atmospheric chemical reactions² and also influence the climate.³ The interest in this reaction in the field of atmospheric science has stimulated renewed research into the mechanism of gas-phase hydration of sulfur trioxide. Recent high-level ab initio molecular orbital calculations^{4–5} and careful experimental studies^{6–8} have revealed that the dominant channel involves two water molecules.⁶ These developments have been summarized in ref 9.

The function of the second H₂O molecule is to assist in the transfer of the proton from the water molecule, which is attacking the S atom, to one of the three O atoms already attached to the sulfur. By acting as an intermediate link in a two-step proton exchange, the second H₂O lowers the barrier for the redistribution of protons in the hydrated SO₃.^{5,9} Participation of ancillary water molecules is already known to facilitate the addition of H₂O to the carbonyl group in aldehydes^{10–12} and CO₂.¹³ Solvent catalysis involving cooperative proton transfer via one or more water molecules has also been postulated for the addition of water to carbonyl bonds in aqueous solution under neutral pH conditions.¹⁴ A similar

mechanism could also accelerate the hydration of SO₃ in solution. However, the product H₂SO₄ is a much stronger acid than carbonic acid or diols. Hence, the excess proton of the H₂O being added can simply remain with the solvent molecule that receives it. The result is a H₂SO₄ molecule already dissociated into ionic HSO₄[–] and H₃O⁺ fragments.

The addition of H₂O to SO₃, therefore, is an elementary example of a chemical process which can be completely altered by solvation. The solvent effect can be drastic enough to prefer products that are different from the neutral species formed in the gas-phase reaction. This motivated us to select this reaction for a computational study that takes into account the molecular details of the solvent. The technique we employ is ab initio molecular dynamics (MD) simulation,¹⁵ originally proposed by Car and Parrinello and therefore also referred to as CPMD. With this MD method the forces on the atoms are obtained from a continuously updated electronic-structure calculation. The details of the motion during reactive encounters as well as the finite-temperature solvent dynamics are described by this approach. This feature makes ab initio MD particularly suitable for the investigation of reactions in solution. Examples of previous applications to solution chemistry can be found in refs 16–18.

The electronic states in our ab initio MD method are determined by a computational approach based on density functional theory (DFT) employing a general gradient approximation (GGA) for the energy functional. The GGA used here is Becke–Lee–Yang–Parr (BLYP).^{19,20} Oxides of sulfur and the related oxy-acids and oxy-anions belong to the more difficult compounds for treatment by quantum chemistry methods. A second objective of our study is, therefore, to evaluate how BLYP performs for this class of molecules. Here we can exploit the accurate molecular orbital (MO) type calculations and experimental data on the gas-phase reactions that have recently become available in the literature.^{4,5} Hence, we have repeated some of the calculations of refs 4 and 5. First

[†] Present address: Department of Physical and Theoretical Chemistry, Vrije Universiteit, NL-1081 HV Amsterdam, The Netherlands.

* To whom correspondence should be addressed. Present address: Department of Chemistry, University of Cambridge, Cambridge, CB2 1EW, U.K.

we will compare our gas-phase results with these data and with experiment, and then we will continue the discussion of the ab initio MD simulation of the reaction in solution.

Methods

The electronic states were computed within the Kohn–Sham formulation of DFT using the BLYP density functional. This GGA functional consists of the local exchange energy of the electrons with the gradient correction according to Becke¹⁹ and the GGA correlation energy expression proposed by Lee, Yang, and Parr.²⁰ The BLYP functional has proved to provide a reasonable description of the hydrogen-bond strength of the water dimer as well as of the local structure and diffusion constant of liquid water under ambient conditions.²¹ The Kohn–Sham equations were solved using the pseudopotential approach.^{15–22} The one-electron wave functions are expanded in a plane–wave basis set, and truncated at a kinetic energy E_{cut} , the value of which will be specified below. Only valence electrons are considered explicitly, and semilocal norm-conserving pseudopotentials were used to account for interactions between the valence electrons and the ionic cores. The pseudopotentials for oxygen and sulfur were generated using the Troullier–Martins procedure.²³ The oxygen potential was generated with a ground-state valence-electron configuration using radii of $r_c = 1.1$ au for both the $l = s$ and $l = p$ term. The sulfur potential was constructed with an excited positively charged valence-electron configuration $s^{1.75}p^{3.25}d^{0.50}$, using radii of $r_c = 1.34$ au for the $l = s, p,$ and d terms. The potentials were transformed into the Kleinman–Bylander form²⁴ with $l = p$ and $l = d$ as the local terms for oxygen and sulfur, respectively. For hydrogen we employed a simple analytic pseudopotential that is essentially a softened Coulomb potential. All calculations were carried out using the CPMD package²⁵ for ab initio electronic-structure and MD calculations (for technical details of the MD algorithms used in CPMD, see also refs 26 and 27).

Results

Gas-Phase Hydration. The quantum chemistry calculations that are the reference for the evaluation of our DFT results of the energetics on the SO_3 hydration reaction are high-level ab initio MO calculations using fourth-order Møller–Plesset perturbation theory (MP4).^{4,5} Hofmann and Schleyer⁴ studied the reaction involving a single water molecule at the RMP4SDQ/6-311+G(2df,p)//RMP2(fu)/6-31+G*+ZPE(RMP2(fu)/6-31G*) level. Morokuma and Muguruma⁵ used MP4SDQ/6-311+G(d,p)//MP2/6-311+G(d,p)+ZPE(HF/6-311+G(d,p)) in a study of the hydration of sulfur trioxide involving both one and two water molecules. Figure 1 schematically shows the geometries of the reactant, transition, and product states found in these studies. The monocomplex $\text{SO}_3 \cdot \text{H}_2\text{O}$ reacts by transferring a single proton from the hydrating water to an oxygen of the SO_3 , whereas $\text{SO}_3 \cdot (\text{H}_2\text{O})_2$ converts into a sulfuric acid–water complex by simultaneously transferring two protons.

Before we discuss the results obtained for the systems in Figure 1 using the DFT methodology outlined in the preceding section, we will give the values of some of the essential parameters in the calculation. The $\text{SO}_3 \cdot \text{H}_2\text{O}$, $\text{SO}_3 \cdot (\text{H}_2\text{O})_2$ complexes and H_2SO_4 molecule were placed in a periodic face-centered cubic box, with periodic image distances of 9.4 Å for the monocomplex $\text{SO}_3 \cdot \text{H}_2\text{O}$ and H_2SO_4 , and 11.2 Å for dicomplex $\text{SO}_3 \cdot (\text{H}_2\text{O})_2$. The plane–wave basis set was truncated at a cutoff energy of $E_{\text{cut}} = 70$ Ry. For these values of box size and energy cutoff, the formation energy of the reaction $\text{SO}_3 + \text{H}_2\text{O} \rightarrow \text{H}_2\text{SO}_4$ converged within 1 kJ/mol, as we

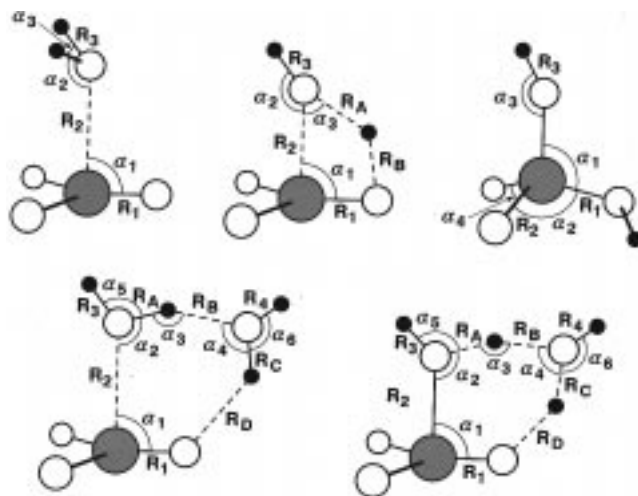


Figure 1. Geometries of $\text{SO}_3 \cdot \text{H}_2\text{O}$, $\text{SO}_3 \cdot \text{H}_2\text{O}^{\text{TS}}$, and H_2SO_4 (upper row), and $\text{SO}_3 \cdot (\text{H}_2\text{O})_2$, and $\text{SO}_3 \cdot (\text{H}_2\text{O})_2^{\text{TS}}$ (lower row). The calculated values of the indicated bond lengths and angles are listed in Tables 1 and 2.

determined by calculating the formation energy using a box size with a periodic image distance of 13.1 Å and a plane–wave energy cutoff of $E_{\text{cut}} = 100$ Ry.

In order to estimate the location of the transition state of the hydration reactions, we assumed the reaction path to be in the subspace of geometries obtained by varying the antisymmetric stretch coordinate associated with the transferred proton(s): $R_{\text{AB}} = R_{\text{A}} - R_{\text{B}}$ for $\text{SO}_3 \cdot \text{H}_2\text{O}$ and $R_{\text{AB}} = R_{\text{A}} - R_{\text{B}}$ and $R_{\text{CD}} = R_{\text{C}} - R_{\text{D}}$ for $\text{SO}_3 \cdot (\text{H}_2\text{O})_2$. We refer to Figure 1 for the definition of the distances $R_{\text{A}}, R_{\text{B}}, \dots$. The energy was determined as a function of the reaction coordinates by simulated annealing: for various fixed values of the reaction coordinate(s) we performed a finite-temperature CPMD simulation during which the temperature was decreased stepwise to approximately 5 K. During this simulation the reaction coordinate was fixed by the method of constraints.^{18,28} We estimate the calculated energy to be within 2 kJ/mol of the true minimal energy. In our calculation of the transition states, we started from the transition-state geometry of ref 4 for $\text{SO}_3 \cdot \text{H}_2\text{O}$ and that of ref 5 for $\text{SO}_3 \cdot (\text{H}_2\text{O})_2$. Subsequently, we calculated the energies of geometries obtained by small variations of the reaction coordinates about the initial geometry.

The zero-point energies (ZPEs) were estimated using values reported in the literature. Reference 4 provided the ZPEs of H_2O , SO_3 , $\text{SO}_3 \cdot \text{H}_2\text{O}$, $\text{SO}_3 \cdot \text{H}_2\text{O}^{\text{TS}}$, and H_2SO_4 , obtained from vibrational frequencies calculated at the RMP2(fu)/6-31G* level. The ZPEs of $\text{SO}_3 \cdot (\text{H}_2\text{O})_2$ and $\text{SO}_3 \cdot (\text{H}_2\text{O})_2^{\text{TS}}$ are not yet available in the literature and were estimated as the sum of three contributions: (i) the ZPEs of $\text{SO}_3 \cdot \text{H}_2\text{O}$ and $\text{SO}_3 \cdot \text{H}_2\text{O}^{\text{TS}}$ (ref 4, RMP2(fu)/6-31G* level), (ii) the ZPE of H_2O (ref 4, RMP2(fu)/6-31G* level), and (iii) the difference of the ZPE of $(\text{H}_2\text{O})_2$ and twice the ZPE of H_2O (ref 29, MP2/aug-cc-pVTZ level). We estimate the accuracy of these approximate ZPEs to be better than 4 kJ/mol.

Tables 1 and 2 list the DFT results for selected geometrical parameters of $\text{SO}_3 \cdot \text{H}_2\text{O}$, $\text{SO}_3 \cdot (\text{H}_2\text{O})_2$, their transition states, and H_2SO_4 , and the tables compare these to experimental values (where available) and to quantum chemistry calculations. Overall, the DFT results are in good agreement with experiment, the intramolecular SO bond lengths showing the largest deviations. The OH bond lengths agree within 0.01 Å, whereas the intramolecular SO bond length for SO_3 in the $\text{SO}_3 \cdot \text{H}_2\text{O}$ and the bonds from S to a hydroxyl O in H_2SO_4 , both labeled R_1 in Figure 1 and Table 1, are overestimated in DFT by 0.02–0.06

TABLE 1: DFT Results for Selected Bond Lengths and Angles of SO₃·H₂O, SO₃·H₂O^{TS}, and H₂SO₄^a

		DFT	RMP2 ^b	MP2 ^c	exptl
SO ₃ ·H ₂ O	R ₁ (SO)	1.448(2)	1.457	1.447	1.4198 ^d
	R ₂ (SO)	2.45(2)	2.453	2.512	2.432 ^e
	R ₈ (OH)	0.976(2)	0.975	0.962	0.965 ^f
	α ₁ (OSO)	95(1)	94.3	93.9	92.6 ^e
	α ₂ (SOH)	107(1)		116.1	103 ^e
	α ₃ (HOH)	105.4(3)	105.9	104.6	104.8 ^f
SO ₃ ·H ₂ O ^{TS}	R ₁ (SO)	1.533(2)	1.539	1.528	
	R ₂ (SO)	1.935(5)	1.896	1.921	
	R ₃ (OH)	0.9803(3)	0.984	0.970	
	R _A (OH)	1.250(2)	1.254	1.236	
	R _B (HO)	1.270(2)	1.274	1.237	
	R _{AB}	-0.020	-0.020	0.001	
	α ₁ (OSO)	80.8(1)	90.8	80.4	
	α ₂ (SOH)	109.2(3)	110.2	110.8	
	α ₃ (SOH)	67.7(2)		66.9	
	α ₄ (OSO)	102.0(5)	101.7		101.3(1.0)
H ₂ SO ₄	R ₁ (SO)	1.633(2)	1.623	1.615	1.574(10)
	R ₂ (SO)	1.441(2)	1.446	1.432	1.422(10)
	R ₃ (OH)	0.981(2)	0.982	0.969	0.97(1)
	α ₁ (OSO)	104.8(2)	108.9	108.9	108.6(5)
	α ₂ (OSO)	104.8(2)	108.9	108.9	108.6(5)
	α ₃ (SOH)	108.4(2)	108.5	108.7	108.5(1.5)
	α ₄ (OSO)	124.2(2)	125.0		123.3(1.0)

^a Definitions of the bonds (angstroms) and angles (degrees) are given in Figure 1. The DFT energies are calculated using the BLYP functional. For comparison the table also lists values obtained experimentally and by (R)MP2 molecular-orbital calculations. The numbers in the row of experimental values for SO₃·H₂O in italic are the gas-phase values for isolated SO₃ and H₂O. ^b Reference 4. ^c Reference 5. ^d Reference 47. ^e Reference 44. ^f Reference 45.

TABLE 2: DFT Results for Selected Bond Lengths and Angles of SO₃·(H₂O)₂ and SO₃·(H₂O)₂^{TS} ^a

	SO ₃ ·(H ₂ O) ₂		SO ₃ ·(H ₂ O) ₂ ^{TS}	
	DFT	MP2 ^b	DFT	MP2 ^b
R ₁ (SO)	1.460(2)	1.452	1.503(1)	1.492
R ₂ (SO)	2.22(2)	2.331	1.865(5)	1.837
R ₃ (OH)	0.976(1)	0.963	0.9775(5)	0.967
R ₄ (OH)	0.973(1)	0.960	0.9768(5)	0.966
R _A (OH)	1.010(2)	0.979	1.386(2)	1.359
R _B (HO)	1.67(1)	1.785	1.115(2)	1.088
R _{AB}	-0.66(1)	-0.806	0.27(1)	0.271
R _C (OH)	0.980(2)	0.965	1.076(3)	1.053
R _D (HO)	2.15(3)	2.108	1.464(2)	1.442
R _{CD}	-1.17(3)	-1.143	-0.39(1)	-0.389
α ₁ (OSO)	95.5(5)	92.1	98.4(2)	95.2
α ₂ (SOH)	104.8(5)	107.8	105.4(4)	106.9
α ₃ (OHO)	166(1)	158.7	156.8(2)	154.0
α ₄ (HOH)	97(1)	91.6	90.8(4)	91.6
α ₅ (HOH)	107.0(2)	105.1	115.4(4)	
α ₆ (HOH)	106.3(2)	105.2	109.6(4)	

^a Definitions of the bonds (angstroms) and angles (degrees) are given in Figure 1. The DFT calculation is based on the BLYP functional. For comparison the values obtained by MP2 molecular-orbital methods are also listed. ^b Reference 5.

Å. Most of the bond angles in SO₃·H₂O and H₂SO₄ are reproduced within 2° by DFT. Exceptions are the orientation α₂ of the OH bond of H₂O in SO₃·H₂O, which differs up to 4° from the experimental values, and the SO–SOH bond angle α₂ in H₂SO₄, which is underestimated by ≈3°.

Regarding the comparison to MP2, the tables show that DFT performs on practically the same level of accuracy for both the minimum-energy configurations and the transition-state geometries. Note that for the elongated SO bonds the discrepancies of the MP2 and DFT results with respect to experiment are similar. The antisymmetric stretch coordinates of the transferred protons, R_{AB} for the monohydrate and R_{AB}, R_{CD} for the dihydrate, agree within 0.02 Å. Other intermolecular bond

TABLE 3: DFT Energies (kJ/mol) of the Sulfur Trioxide–Water Complexes, Their Transition States, and Corresponding Reaction-Barrier Heights (Δ), and H₂SO₄^a

	DFT	RMP4 ^b	MP4 ^c	exptl
SO ₃ ·H ₂ O	-21 (-29)	-33	-35	-54 ^d
SO ₃ ·H ₂ O ^{TS}	78 (76)	80	100	
Δ	99	113	135	
SO ₃ ·(H ₂ O) ₂	-49 (-66)		-65	
SO ₃ ·(H ₂ O) ₂	-18 (-29)		-13	-54 ^d
Δ	31		52	
H ₂ SO ₄	-30 (50)	-86	-58	-93 ± 10 ^e

^a DFT energies are calculated using the BLYP functional and are relative to the sum of the energies of isolated H₂O and SO₃. For comparison the table also lists the values obtained by (R)MP4 molecular orbital calculations, and the experimental value⁴⁶ for sulfuric acid. All values include zero-point energies (see text); the DFT values in parentheses are without zero-point energy correction. The basis-set superposition error in the RMP4 energies, not corrected for in the table, is estimated by Hofmann and Schleyer⁴ to be less than 2 kJ/mol. ^b Reference 4. ^c Reference 5. ^d Reference 8. ^e Reference 46.

lengths can differ by as much as 0.03 Å. For intramolecular bond lengths the discrepancies are smaller, namely ≈0.01 Å. Intramolecular bond angles agree within 3°. For the intermolecular bond angles we find differences with a maximum of 10°. These are the quantities that are most sensitive to the exact path of proton transfer, see, for example, the OSO angle α₁ of SO₃·H₂O^{TS} in Figure 1 (recall that the configuration space of our transition-state search is limited).

The DFT energies for the sulfur trioxide–water complexes, transition states, and product H₂SO₄ are given in Table 3 together with the available experimental values and the results obtained with the MP4 calculations. Whereas the DFT and MP2 descriptions of structure are of comparable quality, the energetics yields a less consistent picture. Stabilization energies of the equilibrium SO₃·H₂O and SO₃·(H₂O)₂ are similar in DFT and MP4. The differences in the range of 10 kJ/mol are not insignificant but are still within the limits of what can be expected considering the complicated nature of the binding of the adduct states, which is intermediate between a chemical bond and intermolecular interaction. The ≈30 kJ/mol underbinding of SO₃·H₂O in DFT with respect to experiment is more serious. The variation of energy barriers in DFT compared to MP4 is also of the order of 10–20 kJ/mol, with DFT again yielding somewhat smaller values. As in ref 5, we find that the energy barrier is significantly lower for the dihydrate than for the monohydrate. Hence, the DFT calculations are consistent with the observation in ref 5 that the energetics of the sulfur trioxide–water complexes are in qualitative agreement with the recent experimental findings^{6,8} that the gas-phase hydration reaction of sulfur trioxide is second order in the water concentration.

From the data in Table 3 it is evident that our DFT calculation has a tendency to reduce energy maxima as well as minima. This leads to an energy profile that is more uniform than those from MP4 and experiment. This equalizing effect is most pronounced for the H₂SO₄ formation energy. The stability of H₂SO₄ with respect to SO₃ and H₂O is underestimated by as much as 60 kJ/mol (i.e., by a factor of 3). The RMP4 formation energy of H₂SO₄ in ref 4 is much better and in almost perfect agreement with experiment. Note, however, that the MP4 calculation in ref 5 also underestimates the formation energy of H₂SO₄ by a significant amount, although not by as much as DFT does. To analyze the disappointing performance of DFT, we start with the observation that basis-set superposition errors are absent from our results. This is the advantage of using a plane–wave basis set. Moreover, remaining limitations of the size and convergence of the basis set applied here (see above)

cannot be responsible for an error of this magnitude. Another source of error in our approach is the use of pseudopotentials. Although the possibility of a bias introduced by insufficient transferability of the pseudopotentials cannot be completely eliminated, the amount of energy that is missing in the formation of H_2SO_4 is too large to be explained by this effect. To support this claim we have verified that a frozen-core molecular orbital DFT calculation based on the same density functional (BLYP) yields a comparable number. Using the ADF code³⁰ with a large basis set,³¹ we obtained a H_2SO_4 formation energy of 27 kJ/mol.

This leaves the approximations underlying the BLYP functional as the main suspect. We have not been able to analyze the possible reason for failure of BLYP in more detail. However, surveying the literature on comparative tests of GGAs, we noticed that a considerable fraction of the systems identified as a bad case in terms of energetics concerns addition reactions. Similar to SO_3 hydration, these reactions involve the transformation of reactants containing bonds of high bond order to products with a larger number of bonds of lower bond order. Examples are the reactions discussed in ref 32. Further discussion of this crucial issue will be deferred to the summary in the last section after presentation of the simulation of the reaction in aqueous solution.

Condensed-Phase Hydration. Next we turn to the main theme of the present work: the effect of a dense aqueous environment on the hydration of sulfur trioxide. In order to study this reaction we performed an ab initio CPMD simulation of a single sulfur trioxide molecule in liquid water at ambient density and a temperature of 300 K. We used a periodic cubic cell containing 20 water molecules and one sulfur trioxide molecule. The density was taken from the density–composition relation for aqueous sulfuric acid of ref 33 (eq A10), which yields a cell size of 8.59 Å for a sulfuric acid–water mixture with a number–density ratio of 1:19. The same plane–wave energy cutoff was taken as in the calculations of the gas-phase systems (i.e., $E_{\text{cut}} = 70$ Ry).

In order to generate an initial configuration, we first performed an MD simulation of several picoseconds (ps) of the $\text{SO}_3/\text{H}_2\text{O}$ mixture using a simple classical force field. This ensured an approximately correct hydrogen-bonded structure for solvent and SO_3 solute. With the final state of the model simulation as input, the MD run was continued for about 1 ps using ab initio CPMD, with the inversion plane of SO_3 fixed to 180° . During this run the local water structure around the SO_3 was allowed to relax under the influence of the ab initio forces. The inversion-plane constraint was imposed to prevent immediate reaction of SO_3 with H_2O in this equilibration phase. The temperature was controlled by a Nosé thermostat with a target average of 300 K (for the implementation of the Nosé thermostat in CPMD, see refs 26 and 27).

We prepared two independent configurations according to this procedure. These samples were used as initial configurations for two ab initio CPMD simulations of the $\text{SO}_3/\text{H}_2\text{O}$ mixture for approximately ≈ 3 ps. In both runs we observed a rapid conversion of the sulfur trioxide molecule and two neighboring water molecules into a $\text{HSO}_4^- - \text{H}_3\text{O}^+$ contact ion pair. Attack by a nearby solvent molecule starts within 0.2 ps from the beginning of the run, indicating that the energy barrier for the reaction, if present at all, is of the order of the thermal energy k_{BT} (≈ 2.5 kJ/mol). Figure 2 shows how the reaction proceeds in three snapshots of the trajectory of one of the two CPMD simulations. Initially, a water molecule orients its oxygen toward the sulfur into a configuration similar to that of

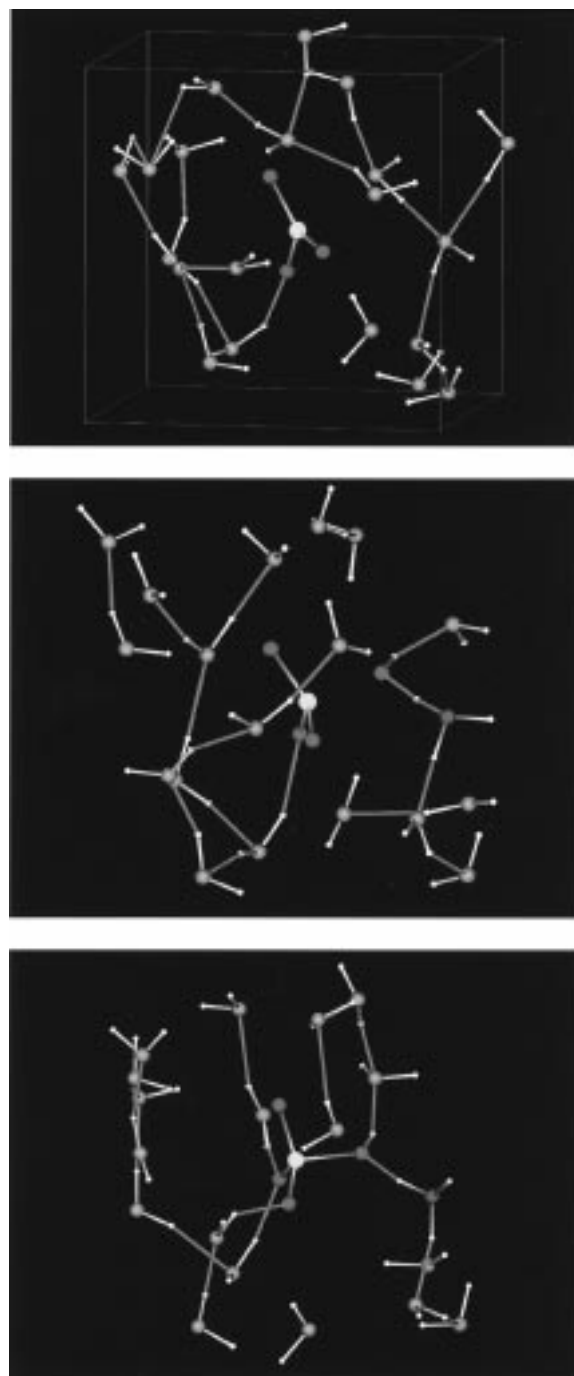


Figure 2. Three snapshots of the trajectory of an ab initio molecular dynamics simulation of the addition of water to sulfur trioxide in aqueous solution. Hydrogen, oxygen, and sulfur atoms are white, blue, and yellow, respectively. When an O atom is bonded to S it is colored red. The green lines represent hydrogen bonds, whereas the other lines indicate intramolecular bonds. The long, thin red lines mark the edges of the cubic simulation box. Time is measured relative to an initial configuration equilibrated with constraints on the sulfur trioxide inhibiting reaction. (Top): Time is 30 fs. A water molecule above the sulfur trioxide turns its oxygen toward the sulfur. (Middle): Time is 140 fs. This water molecule, with its oxygen (red) now oriented toward the sulfur, is approaching the sulfur trioxide molecule. Simultaneously with the nucleophilic attack, one of the protons of the H_2O is passed to the oxygen (pink) of a second water molecule. (Bottom): Time is 190 fs. A new sulfur–oxygen bond has formed, converting the sulfur trioxide into a sulfate anion. The hydrating water molecule has transferred a proton to the second water molecule, creating a hydronium ion that forms a contact ion pair with the sulfate anion.

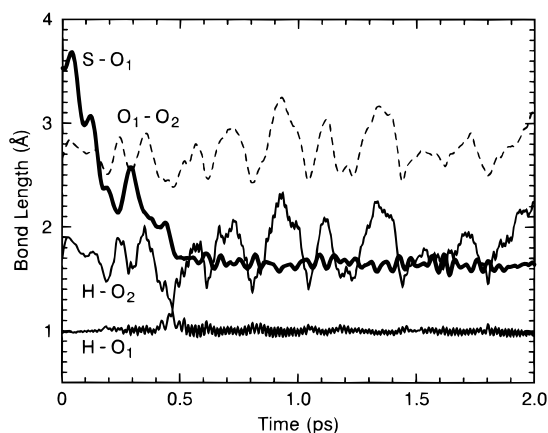


Figure 3. Time evolution of distances between reactive atoms in the addition reaction of sulfur trioxide in liquid water. The proton transferred from the reactive water molecule to a second water molecule is indicated by H. O₁ is the oxygen of the reactive water molecule; O₂ is the oxygen of the second water molecule; the sulfur atom is labeled S.

the gas-phase monohydrate (see Figure 1). Subsequently, this water molecule approaches the sulfur atom, and an oxygen–sulfur bond is formed. Simultaneously, one of the protons of the reactive water molecule is transferred along a hydrogen bond to a neighboring water molecule. The product state is a contact ion pair consisting of a hydrogen sulfate HSO₄[−] and a hydronium ion H₃O⁺. Hence, from this spontaneous and almost instant reaction in the CPMD simulation, it must be concluded that a sulfur trioxide–water complex similar to the adduct found in the gas phase is not stable in aqueous solution. Solvation strongly increases the acidity of the complex, inducing immediate deprotonation.

The concerted nature of the formation of the oxygen–sulfur bond and the proton transfer are illustrated in Figure 3, where the relative distances of the atoms participating in the reaction are plotted as a function of time. Following the trajectories from time zero, we see a water oxygen atom O₁ approaching the sulfur atom from a SO distance of $d_{SO_1} = 3.5$ Å. This initial distance is typical for intermolecular interactions. The almost continuous and rapid decrease of d_{SO_1} is the signature of the nucleophilic attack in progress. When, after 0.4 ps, d_{SO_1} is close to attaining the final equilibrium SO bond length of ≈ 1.8 Å, a proton that until then had been attached to O₁ changes its bonding site to atom O₂ of a nearby H₂O, turning this molecule into a hydronium ion. Note that during the proton transfer, which is completed in less than 0.2 ps, the oxygen–oxygen distance $d_{O_1-O_2}$ distance is small, ≈ 2.4 Å. For protonated water dimers it is known that for such short oxygen–oxygen distances the hydrogen-bonded proton is located midway between the oxygens of the two water molecules, and is confined in a single potential well (see, e.g., ref 34). Applying this distance criterion to the condensed phase, we infer that, during transfer, the proton also moves in a single well. This would minimize the role of tunneling and could be an argument to justify the total neglect of nuclear quantum effects in the MD simulation in which all atoms, including H atoms, are treated classically.

The sequence of events and the fast rate at which they proceed suggest that the addition occurs as soon as a water molecule in the first coordination shell of the sulfur center has the appropriate orientation. This would imply that the rate-limiting step is the reorientation time of a water molecule (i.e., the time it takes for the hydrating molecule to orient its oxygen towards the sulfur atom). The reorientation time in BLYP water, as determined by the ab initio MD study of the pure liquid investigated in ref

21, is approximately 3 ps (the experimental value measured by NMR is 2 ps³⁵). This period of time must be interpreted as an upper limit for the reaction time. The considerably shorter value of ≈ 0.5 ps observed in our two samples could be explained as resulting from favorable orientations of the water molecules in the initial state. Alternatively, the short time scale might be an indication that there is a significant force driving the reaction (i.e., that the reaction is strongly exothermic).

The monocomplex SO₃·H₂O in water has also been studied by ab initio MO.⁴ This calculation, using the self-consistent reaction field (SCRF) method to approximate the effect of the aqueous environment, predicted that solvation increases the binding energy of the monocomplex by as much as 49.8 kJ/mol. The enhanced stability is reflected in a significant reduction (0.63 Å) of the intermolecular SO distance. The conclusion drawn in ref 4 that complexation is energetically more favorable in solution is not contradicted by our results. What the CPMD simulation demonstrates is that such an adduct is unstable with respect to the hydrogen sulfate anion. Clearly, the SCRF calculation can give only a limited picture of the behavior of sulfur trioxide in water owing to its continuum description of the aqueous environment. In particular, it is not able to account for the dissociation of H₂SO₄ found in the CPMD simulation. However, the SCRF trend of a decreasing bond length and an increasing stability of solvated sulfur–trioxide water complexes seems qualitatively consistent with the high reactivity of these species observed in the CPMD simulation.

Summary

Using ab initio molecular dynamics methods we have compared the mechanism of the reaction of water and sulfur trioxide in liquid water to the gas-phase process. The simulation showed that reaction path and energetics in the two phases are dramatically different. As can be expected in view of the strong acidity of sulfuric acid, formation of a product H₂SO₄ molecule is avoided in aqueous solution. Instead, sulfur trioxide is directly converted into a hydrogen sulfuric acid anion. The main result of the simulation is the observation that SO bond formation and the transfer of a proton by the attacking H₂O molecule to the solvent are concerted events and occur on a sub-picosecond time scale. The spontaneous and fast reaction dynamics is an indication that solvation effects have completely eliminated the barrier for hydration. An interesting question that remains to be resolved is the minimum number of water molecules needed in a gas-phase cluster to achieve a similar reduction of the barrier.

A second, equally important objective of this paper was more technical. The implementation of the Kohn–Sham method in our ab initio MD code has certain special features which are adapted to the determination of electronic states in extended (periodic) systems. This involves, in particular, the use of plane–wave basis sets and pseudopotentials for the core electrons. GGAs, such as BLYP used here, can be included in such an approach with negligible additional computational cost compared to the corresponding local density approximation (LDA) calculation and are now standard in ab initio MD. Originally developed for typical problems in solid-state physics, the number of applications to calculate reaction energies in finite (gas phase) systems is still limited. Therefore, a thorough evaluation of the performance in the case of a difficult chemical process, such as the addition reaction considered here, may yield useful information for future ab initio MD studies of chemical reactions. The conclusions of this investigation are not positive

in every respect. The geometries obtained for the gas-phase complexes $\text{SO}_3 \cdot \text{H}_2\text{O}$, $\text{SO}_3 \cdot (\text{H}_2\text{O})_2$, and the H_2SO_4 product are in good agreement with the results of experiment and of high-level correlated molecular orbital methods.^{4,5} However, the energetics was found to be severely in error. The stability of the compounds is systematically underestimated. In particular, the energy for the formation H_2SO_4 from SO_3 and H_2O is too small by almost a factor of 3. We have verified that a bias of this magnitude is not caused by restrictions in size of our basis set or insufficient transferability of pseudopotentials. Therefore, we concluded that the origin of these discrepancies must be related to approximations implicit in the BLYP functional.

Addition reactions, indeed, are a stringent test for the calculation of energies in DFT. Splitting of high-order bonds into bonds of lower order leads to major rehybridization of the atomic valence orbitals. However, as pointed out in ref 36, the response of the exchange energy to changes in orbital symmetry is not well described by either LDA or GGA. In fact, in order to account for these nonlocal exchange effects, extension of the GGA functional with an exact (Kohn–Sham) exchange component may well be the only solution.^{37–39} A popular hybrid functional mixing exact exchange with B88 exchange and LYP correlation is B3LYP (see, e.g., ref 38). Unfortunately, evaluation of the energy of Slater determinants consisting of Kohn–Sham orbitals expanded in plane waves is a computationally very expensive operation, and is, in practice, not feasible in ab initio MD applications. Exclusion of hybrid functionals from the list of density function options in ab initio MD code is an indirect consequence of the use of a plane basis set and can, therefore, be considered a serious drawback of this approach.

A further complication is that the prediction of relative exchange energies is probably not the only source of error in the BLYP treatment of the thermochemistry of addition reactions. It has been suggested³² that correlation effects could also be responsible. Because, in the course of the addition process, the two electron pairs making up a double bond are spatially separated, the correlation energy between parallel spins is particularly sensitive to this redistribution of charge. The LYP functional is clearly not the best choice to determine the change in parallel spin correlation because it has been parametrized using the total energy of the helium atom, which contains only antiparallel spins. This argument was one of the main motivations for the generalization of the LYP functional proposed in ref 32. A functional combining all of these effects (i.e., exact exchange mixing and distinct treatment of dynamical parallel and opposite spin correlations), is the recent one-parameter (B1) hybrid developed by Becke in ref 39. The nonempirical approach to density functionals of Perdew et al. also heads in this direction.⁴⁰

Which fraction of the missing 60 kJ/mol in the BLYP formation energy of H_2SO_4 from SO_3 and water is due to exchange and which to correlation effects remains to be resolved by careful comparison of the results of a number of functionals. However, the perhaps somewhat extreme case of sulfuric acid demonstrates that BLYP, which has become one of the preferred functionals in ab initio MD applications, can fail by an unacceptable margin in the calculation of reaction energies. This leads us to the urgent recommendation to the ab initio MD community that elimination of the technical difficulties inhibiting the implementation of hybrid functionals be made a priority in the further development of the ab initio MD method. On the other hand, the qualitative conclusions of the simulation study of the bulk hydration reaction are not completely invalidated by the underestimation of the reaction energy. The BLYP

results for the barriers for addition in the gas phase were found to be considerably more reliable than the final energy of the product. Therefore, a larger product formation energy can only enhance the tendency toward spontaneous and concerted reaction dynamics as observed for the simulation in liquid.

References and Notes

- (1) Pruppacher, H. R.; Klett, J. D. *Microphysics of Clouds and Precipitation*; Reidel: Dordrecht, 1980.
- (2) Abbatt, J. P. D.; Molina, M. J. *Annul Rev. Energy Environ.* **1993**, *18*, 1.
- (3) Charlson, R. J.; et al. *Science* **1992**, *255*, 423.
- (4) Hofmann, M.; v. R. Schleyer, P. *J. Am. Chem. Soc.* **1994**, *116*, 4947.
- (5) Morokuma, K.; C. Muguruma, C. *J. Am. Chem. Soc.* **1994**, *116*, 10316.
- (6) Kolb, C. E.; et al. *J. Am. Chem. Soc.* **1994**, *116*, 10314.
- (7) Phillips, J. A.; Canagaratna, M.; Goodfriend, H.; Leopold, K. R. *J. Phys. Chem.* **1995**, *99*, 501.
- (8) Lovejoy, E. R.; Hanson, D. R.; Huey, L. G. *J. Phys. Chem.* **1996**, *100*, 19911.
- (9) Stuedel, R. *Angew. Chem., Int. Ed. Engl.* **1995**, *34*, 1313.
- (10) Bell, R. P.; Millington, J. P.; Pink, J. M. *Proc. R. Soc. London, Ser. A* **1968**, *303*, 1.
- (11) Williams, I. H.; et al. *J. Am. Chem. Soc.* **1983**, *105*, 31.
- (12) Wolfe, S.; et al. *J. Am. Chem. Soc.* **1995**, *117*, 4240.
- (13) Nguyen, M. T.; Ha, T.-K. *J. Am. Chem. Soc.* **1984**, *106*, 599.
- (14) Eigen, M. *Discuss. Faraday Soc.* **1965**, *39*, 7.
- (15) Car, R.; Parrinello, M. *Phys. Rev. Lett.* **1985**, *55*, 2471.
- (16) Tuckerman, M.; Laasonen, K.; Sprik, M.; Parrinello, M. *J. Phys. Chem.* **1995**, *99*, 5749.
- (17) Tuckerman, M.; Laasonen, K.; Sprik, M.; Parrinello, M. *J. Chem. Phys.* **1995**, *103*, 150.
- (18) Curioni, A.; et al. *J. Am. Chem. Soc.* **1997**, *119*, 7218.
- (19) Becke, A. D. *Phys. Rev. A* **1988**, *38*, 3098.
- (20) Lee, C.; Yang, W.; Parr, R. G. *Phys. Rev. B* **1988**, *37*, 785.
- (21) Sprik, M.; Hutter, J.; Parrinello, M. *J. Chem. Phys.* **1996**, *105*, 1142.
- (22) Galli, G.; Pasquarello, A. In *Computer Simulation in Chemical Physics*; Allen, M. P., Tildesley, D. J., Eds.; NATO ASI Series C 397; Kluwer: Dordrecht, 1993; p 261.
- (23) Troullier, N.; Martins, J. L. *Phys. Rev. B* **1991**, *43*, 1993.
- (24) Kleinman, L.; Bylander, D. M. *Phys. Rev. Lett.* **1982**, *48*, 1425.
- (25) Hutter, J.; Parrinello, M. CPMD Code, 1995, Version 2.5, developed by J. Hutter and the group of numerical intensive computing at the IBM Zurich Research Laboratory and M. Parrinello's group at MPI in Stuttgart, Germany.
- (26) Tuckerman, M. E.; Parrinello, M. *J. Chem. Phys.* **1994**, *101*, 1302.
- (27) Tuckerman, M. E.; Parrinello, M. *J. Chem. Phys.* **1994**, *101*, 1316.
- (28) Ciccotti, G.; Ferrario, M.; Hynes, J. T.; Kapral, R. *Chem. Phys.* **1989**, *129*, 241.
- (29) Xanthreas, S. S.; Dunning, T. H. *J. Chem. Phys.* **1993**, *99*, 8774.
- (30) ADF 2.2.2 Theoretical Chemistry; Vrije Universiteit: Amsterdam, The Netherlands (see: refs 41–43).
- (31) Molecular orbitals were expanded in a uncontracted triple- ζ Slater-type basis set augmented with 2p and 3d polarization functions for H and 3d and 4f polarization functions for O and S. The cores were kept frozen.
- (32) Proynov, E. I.; Ruiz, E.; Vela, A.; Salahub, D. R. *Int. J. Quantum Chem., Quantum Chem. Symp.* **1995**, *29*, 61.
- (33) Carlsaw, K. S.; Clegg, S. L.; Brimblecombe, P. *J. Phys. Chem.* **1995**, *99*, 11557.
- (34) Tuckerman, M. E.; Marx, D.; Klein, M. L.; Parrinello, M. *Science* **1997**, *275*, 817.
- (35) Jonas, J.; DeFries, T.; Wilber, D. J. *J. Chem. Phys.* **1976**, *65*, 582.
- (36) Gunnarson, O.; Jones, R. D. *Rev. Mod. Phys.* **1991**, *61*, 689.
- (37) Becke, A. D. *J. Chem. Phys.* **1993**, *98*, 5648.
- (38) Johnson, B.; Gill, P. M. W.; Pople, J. A. *J. Chem. Phys.* **1993**, *98*, 5612.
- (39) Becke, A. D. *J. Chem. Phys.* **1996**, *104*, 1040.
- (40) Perdew, J. P.; Ernzerhof, M.; Burke, K. *J. Chem. Phys.* **1996**, *105*, 9982.
- (41) Baerends, E. J.; Ellis, D. E.; Ros, P. *Chem. Phys.* **1973**, *2*, 42.
- (42) te Velde, G.; Baerends, E. J. *J. Comput. Phys.* **1992**, *99*, 84.
- (43) Guerra, C. F.; et al. In *Methods and Techniques in Computational Chemistry*; Clementi, E., Corongiu, G., Eds.; STEF: Cagliari, 1995; Chapter 8, pp 305–395.
- (44) Kaldor, A.; Maki, A. G. *Mol. Struct.* **1973**, *15*, 123.
- (45) Harmony, M. D.; et al. *J. Phys. Chem. Ref. Data* **1979**, *8*, 619.
- (46) Case, M. W.; et al. *J. Phys. Chem. Ref. Data* **1985**, *14*.